Evaluation of an industrial CFD code for LES applications

By Dochul Choi†, Dilip Prasad†, Meng Wang AND Charles Pierce

The feasibility of using an industrial compressible CFD code for large eddy simulations (LES) is evaluated. Dynamic subgrid scale (SGS) models developed at CTR have been implemented into the code and tested in a fully developed turbulent channel flow. In order to evaluate the effects of the SGS model compared with the numerical dissipation inherent in the upwind-biases schemes, computations without any SGS model were also carried out. It is found that the effect of dynamic SGS model decreases with increasing numerical dissipation (low order schemes). The 9th and 11th order schemes have relatively small numerical dissipation, and thus the dynamic SGS model plays useful role. In addition, a wall model was implemented in conjunction with LES. Although the velocity profile obtained with the wall model agrees well with the full LES solution, the magnitude of the pressure fluctuation is found to be overpredicted.

1. Introduction

There is an increasing demand for high fidelity, unsteady CFD capabilities for such applications as turbulence and transition modeling, flow control, aero-acoustics, and combustion system dynamics. Conventional Reynolds Averaged Navier Stokes (RANS) solvers based on various turbulence models often fail to capture unsteady flow physics accurately. This is not surprising in view of the fact that most of these models were developed with the goal of solving steady flow problems. Alternative methods are needed for unsteady CFD analyses in industrial applications.

As computer power becomes more affordable, Large Eddy Simulation (LES) has emerged as a viable and powerful alternative tool in turbulence computations. In recent years, LES has been applied to an increasing number of problems of engineering relevance. This was made possible through the use of parallel computing over under-utilized distributed machines in an industry setting and the availability of relatively cheap processors. The challenge in carrying out LES is that a three-dimensional, unsteady calculation must be carried out on a grid capable of resolving the larger scales of the motion; for flow geometries and Reynolds numbers of engineering interest, this implies that the grid is usually large. Hence, the CPU time required is substantially larger than that for an analogous RANS calculation.

The objective of the present study, carried out as part of the 2000 CTR Summer Program, is to evaluate an industrial CFD code for LES applications. Dynamic subgrid scale (SGS) models developed at CTR were implemented into the code, which was then tested by application to a fully developed channel flow. A significant drawback of contemporary LES methods is the need for a fine grid spacing in the neighborhood of the wall, which leads to prohibitively expensive computations in realistic applications. We attempted to

† United Technologies Research Center, East Hartford, CT 06108

address this issue in this investigation by using a wall model that relieves the grid requirement in the wall region. It is shown that the results obtained by such a treatment show a higher level of wall pressure spectrum.

2. Code description

Over the last few years, LES capability has been added to an existing Euler/RANS code at United Technologies Research Center. This code, called UTNS (**U**pwind-biased **T**ime-dependent **N**avier-Stokes **S**olver), solves the compressible flow equations in conservative form in generalized curvilinear coordinates. The momentum equations are solved together with the continuity and energy equations in a fully coupled, vector form. Spatial differencing is accomplished using finite volumes with upwind biasing. The order of accuracy of the scheme ranges from the first to the 11th order (upwinded) for the convection terms and the second order central differencing for the diffusion terms. Furthermore, there is also an option for second order central differencing for the convection terms which eliminates numerical damping. Temporal advancement is achieved using second order backward differencing with a dual time step, one for physical time step and the other for numerical time step (used as an under relaxation parameter) for sub-iterations. The sub-iteration is carried out using a scalar, implicit, approximate factorization scheme. A third order Runge-Kutta explicit scheme is optional.

The original LES code, developed from the unsteady RANS code, has a simple Smagorinsky subgrid scale (SGS) model with the van Driest wall damping function. The code has been applied to jet-in-cross flows, flows behind flame holders, flows in swirling combustors, and transonic jet mixing. In all of the cases considered thus far, the flows are dominated by large-scale unsteady structures, with relatively small contributions from small scale eddies generated near solid boundaries (Madabhushi *et al.* 1997, Choi *et al.* 1999).

3. Dynamic subgrid scale model

Although the Smargorinsky model is widely used for LES, it has some limitations, the most crucial one being that the model constant needs to be adjusted depending on the flow. Moin *et al.* (1991) have developed a dynamic SGS model for compressible flows by generalizing the model of Germano *et al.* (1991). This procedure uses two filters, a grid filter and test filter (typically twice the grid filter width), to find the optimum model constant as a function of time and position, using a least squares technique (minimizing the difference between the closure assumption and resolved stresses) (Lilly 1992). In LES for compressible flows, density-weighted (Favre) filtering is typically employed. Recently, Boersma & Lele (1999) proposed a standard averaging technique without density weighting. This averaging results in the appearance of extra unknowns which are modeled by a procedure similar to that used for the dynamic SGS model. One of the advantages of this model is the emergence of an SGS mass flux term in the filtered continuity equation, which may help in controlling high wave number numerical instabilities. Following Boersma & Lele (1999), the governing equations of mass, momentum, and energy conservation may be cast into the form

$$\frac{\partial \overline{\rho}}{\partial t} + \frac{\partial \overline{\rho}\,\overline{u}_i}{\partial x_i} = -\frac{\partial}{\partial x_i}\left(\overline{\rho u_i} - \overline{\rho}\,\overline{u}_i\right), \tag{3.1}$$

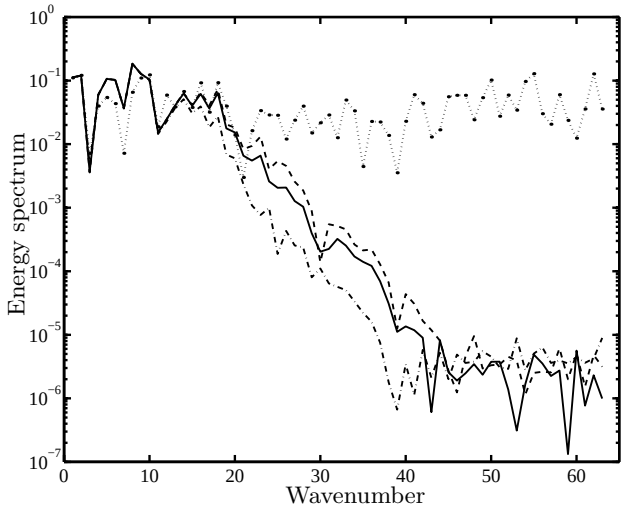

FIGURE 1. Wavenumber spectra of velocity fluctuations based on one dimensional Euler analysis: central differencing (⋯⋯), 9th order (– – –), 7th order (———), and 5th order (—·—).

$$\frac{\partial \overline{\rho}\,\overline{u}_i}{\partial t} + \frac{\partial \overline{\rho}\,\overline{u}_i\,\overline{u}_j}{\partial x_j} = -\frac{\partial \overline{p}}{\partial x_i} + \frac{\partial \overline{\sigma}_{ij}}{\partial x_j} - \frac{\partial}{\partial x_i}\left(\overline{\rho u_i u_j} - \overline{\rho}\,\overline{u}_i\,\overline{u}_j\right) - \frac{\partial}{\partial t}\left(\overline{\rho u_i} - \overline{\rho}\,\overline{u}_i\right), \qquad (3.2)$$

$$\frac{\partial \overline{E}}{\partial t} + \frac{\partial}{\partial x_i}\left(\overline{E}\,\overline{u}_i + \overline{u}_i\overline{p}\right) = -\frac{\partial q_i}{\partial x_i} + \frac{\partial}{\partial x_i}\left(\overline{u}_i\overline{\sigma}_{ij}\right) - \frac{\partial}{\partial x_i}\left(\overline{Eu_i} - \overline{E}\overline{u}_i + \overline{pu_i} - \overline{p}\overline{u}_i\right) \qquad (3.3)$$

where $E = \rho T/\gamma + \rho u_i u_i/2$ is the total energy, the stress tensor $\overline{\sigma}_{ij}$ is defined by

$$\overline{\sigma}_{ij} = \overline{\mu}\left[\frac{\partial \overline{u}_i}{\partial x_j} + \frac{\partial \overline{u}_j}{\partial x_i} - \frac{2}{3}\frac{\partial \overline{u}_k}{\partial x_k}\delta_{ij}\right],$$

and the heat flux $q_i = -\overline{k}\frac{\partial \overline{T}}{\partial x_i}$. The last terms on the right-hand side of the mass and momentum conservation equations are the additional terms arising from the standard averaging rather than density weighted averaging. Both models have been implemented into the UTNS-LES code.

4. Implications of upwinding

In order to examine the numerical characteristics of the upwind scheme, a test case was formulated. It is based on the one-dimensional compressible Euler equations solved using 5th and 7th order upwind biased spatial differencing. The 2nd order central differencing scheme is also used to provide a reference behavior. The calculation starts with random fluctuations at every grid point and advances in time. 128 uniformly-spaced grid points and periodic boundary conditions are used. Since there are no diffusion terms present, the level of the fluctuation should remain the same as that of the initial perturbations. Figure 1 shows the kinetic energy spectra as a function of wave number. The results obtained from the central differencing scheme without any artificial damping show that the level remains the same as the initial values. On the other hand, the results obtained from the upwinding scheme show that the energy at high wave numbers is damped. All the curves shown in Fig. 1 are obtained at the 500th time step, which correspond to 16 acoustic time units based on the domain length and the sound speed of the initial state.

Since the resolved stresses of motion between the test scale and grid scale are used to determine the model constant for the dynamic SGS model, the high wave number solution needs to be computed accurately. Note that most of the dynamic SGS applications at CTR are based on the central differencing scheme for incompressible flow. This scheme is energy conserving and hence free of numerical dissipation. For compressible flows, we cannot identify an energy conserving scheme. Therefore, a new method of estimating the model constant, perhaps by using information at lower wavenumber, may be required. Further research on the dynamic SGS model for an upwind type of scheme is needed to generalize the model for application to industrial CFD codes.

5. Fully developed channel flow

As a test case, we considered a fully developed channel flow with a Reynolds number of 180 based on friction velocity and channel half-width. The problem was solved using 32 grid points in the streamwise and spanwise directions and 64 grid points in the wall-normal direction, covering a domain of $4\pi H \times \frac{4}{3}\pi H \times 2H$, where H is the channel half-width. The cell sizes in the flow and spanwise directions are 72 and 24 wall units respectively, while in the shear (wall-normal) direction, they vary from 1 to 13. The physical time step was 50 in wall units. The calculated results are compared with the result obtained using a CTR-developed LES code for incompressible flow using the same grid.

In order to use the periodic boundary conditions in the streamwise direction, two extra source terms are added to the axial momentum equation: (1) the difference between a target flow rate and integrated computed flow rate, and (2) a total drag force. The purpose of this is to fix the Reynolds number and to eliminate any streamwise pressure gradient. Note that once the solutions reach a statistically steady state, the first forcing term vanishes. The LES calculation starts with a fully developed laminar profile with random number fluctuations of up to 10% the initial velocity. Since the basis for comparison is the incompressible solution, the Mach number in the compressible case was set to a value less than 0.2. Favre-averaged version of the dynamic SGS model was used for the test calculation with high-order upwinding schemes (Wake and Choi 1995). Figure 2 shows the mean axial velocity profiles obtained using the 5th, 7th, and 9th order upwinding schemes. Two calculations, one with the dynamic SGS model and the other without any SGS model, were made with each scheme. The aim was to evaluate the effect of the dynamic SGS model in the presence of numerical dissipation. With the 5th order scheme, there is little difference between two calculations. As the order of the scheme is increased and numerical dissipation decreases, the difference between two solutions increases. The dynamic SGS model seems to be overwhelmed by the numerical dissipation of the low-order schemes. When a scheme of 11th order is used, comparison with the CTR-LES code result, shown in Fig. 3, is observed to be very good; the case without any SGS model shows more mixing in the log region as expected. The profiles of Reynolds shear stress are compared in Fig. 4, where the SGS model used in the 11th order scheme is shown to improve the solution.

Attempts were made to use central differencing without artificial damping but were unsuccessful owing to numerical instability caused by odd-even decoupling. For the central difference case, the standard LES filtered equations of Boersma & Lele (1999) were used as well, but they also failed to produce a statistically steady solution. Note that, using the central differencing without damping, we also considered two-dimensional calculations starting from the similar initial condition as used for the LES and found that

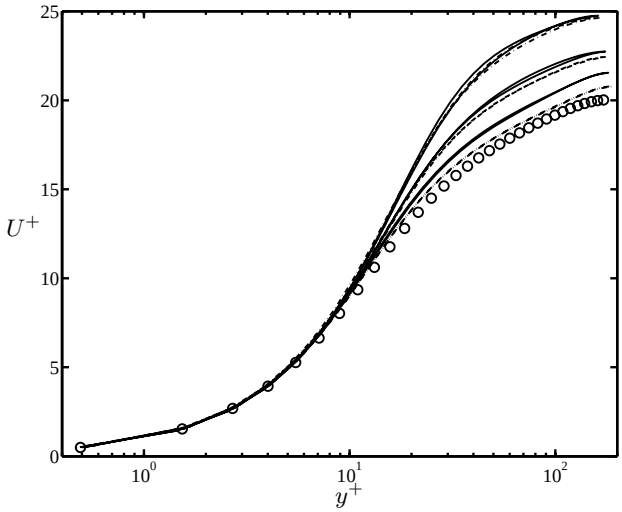

FIGURE 2. Mean velocity profiles obtained using 5th, 7th, and 9th order upwinding schemes (top to bottom) compared with solution from CTR-LES code (○). Solid lines represent computations with SGS model; dashed lines represent those without any SGS model.

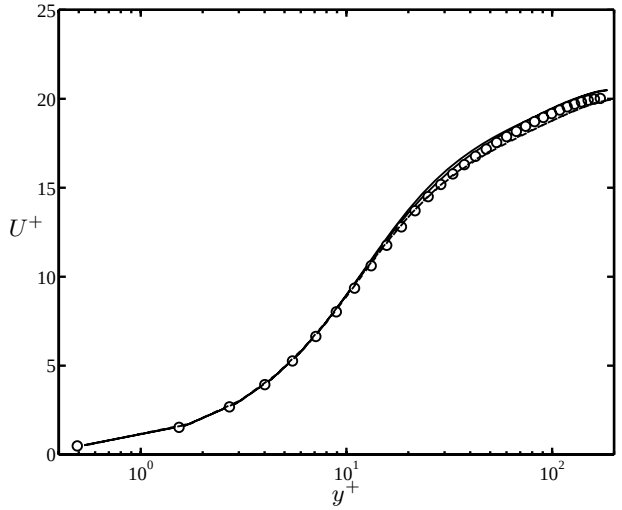

FIGURE 3. Mean velocity profiles obtained using 11th order upwinding scheme compared with solution obtained from CTR-LES code (○). Solid line represents computations with SGS model; dashed line represents those without any SGS model.

the solution reached the steady state and, therefore, became a laminar solution. Thus the presence of three-dimensionality appears to have caused the solution to become unstable.

6. LES with wall model

In order to use LES in practical engineering problems, the stringent grid resolution requirement for high Reynolds number flows in the near wall region needs to be relieved. Wang (1999) reported a factor of 10 reduction in CPU time in an LES for a trailing-

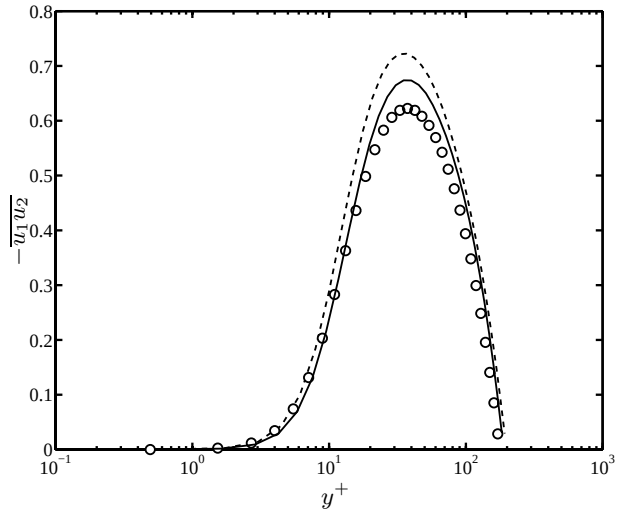

FIGURE 4. Reynolds shear stress profiles obtained using 11th order upwinding scheme compared with solution obtained from CTR-LES code (○). Solid line represents computations with SGS model; dashed line represents those without any SGS model.

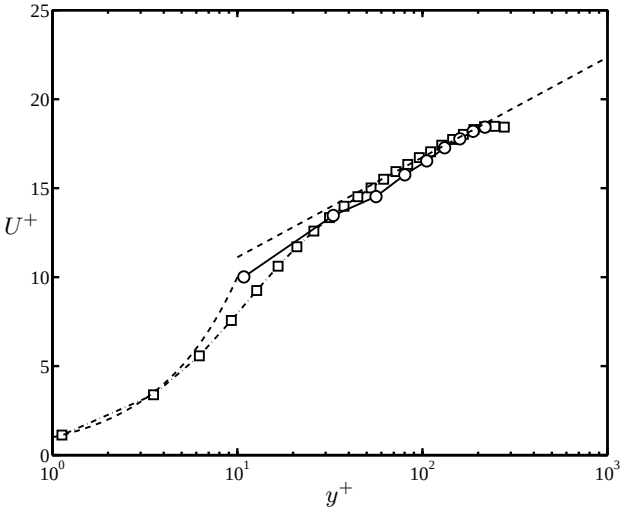

FIGURE 5. Comparison of velocity profiles obtained using LES with wall model (○) and full LES (□).

edge flow using an approximate wall boundary treatment proposed by Cabot and Moin (2000) for incompressible flow. This simple wall model was expanded to the compressible flow equations. The model equations are based on boundary layer approximation of the two tangential direction momentum equations. Modifying the formulation described by Wang (1999) for compressible flow, these equations are integrated from the wall to the first off-wall cell (at a distance δ) according to:

$$\frac{\partial}{\partial x_2}\left(\mu + \mu_t\right)\frac{\partial u_i}{\partial x_2} = F_i, \tag{6.1}$$

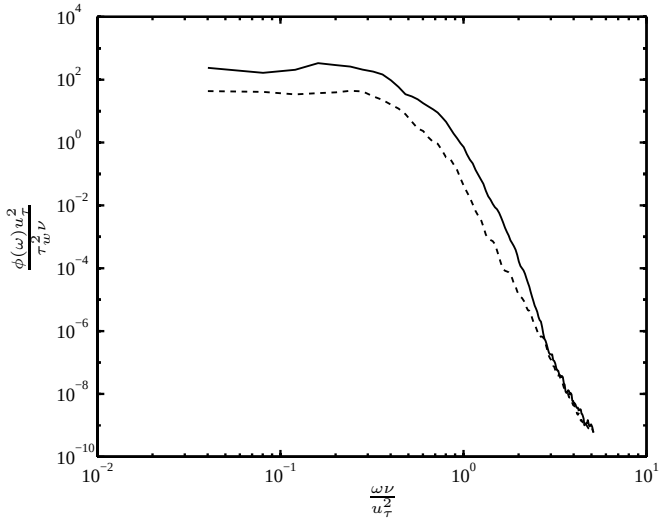

FIGURE 6. Comparison of surface pressure frequency spectra obtained using LES with wall model (———) and full LES (- - - -).

from which the wall shear stress, τ_{wi} is determined to be

$$\tau_{wi} = \mu \left.\frac{\partial u_i}{\partial x_2}\right|_{\text{wall}} = \left[\int_0^\delta \frac{\mathrm{d}x_2}{\mu + \mu_t}\right]^{-1} \left\{u_{\delta i} - \int_0^\delta \frac{F_i x_2}{\mu + \mu_t}\mathrm{d}x_2\right\}. \tag{6.2}$$

The turbulent eddy viscosity μ_t is modeled by

$$\mu_t = \kappa\rho u_\tau d_n \left[1 - \exp\left(-\frac{\rho u_\tau d_n}{A\mu}\right)\right]^2, \tag{6.3a}$$

where d_n is the distance to the wall, $\kappa = 0.4$ is the von Karman constant, and $A = 19$. The forcing term must, in general, be determined according to

$$F_i = \frac{\partial p}{\partial x_i} + \frac{\partial(\rho u_i)}{\partial t} + \frac{\partial(\rho u_i u_j)}{\partial x_j}; \tag{6.3b}$$

here we use the somewhat crude approximation, $F_i = 0$, the so-called "stress-balance model". The calculated wall shear, τ_{wi}, is then used as a boundary condition for the momentum equations in LES. Figure 5 shows the velocity profile compared to the result obtained from a full LES calculation. With the wall model, the number of grid points in the shear direction is reduced to 32 from 64 while the number of grid points in other directions is kept the same. Note that the actual saving in a real application of LES with wall model will come from reductions in axial and spanwise grid points as well. The profiles agree well with each other. In Fig. 6, the frequency spectra of wall pressure fluctuation from the two calculations are examined. We observe that the simulation employing the wall model overpredicts the magnitude of the pressure fluctuation, and this is similar to the behavior reported by Wang (1999); evidently, further study is needed to improve this approximate formulation.

7. Summary

The feasibility of using an industrial compressible CFD code, UTNS, for LES has been evaluated. This was done using a CTR-developed dynamic SGS model in a simple fully developed turbulent channel flow at a Reynolds number of 180, based on the friction velocity and channel half width. In order to evaluate the effect of the SGS model in the presence of numerical dissipation due to upwinding, a computation without any SGS model was also carried out. Calculations were carried out using upwind-biased schemes of up to the 11th order, and the velocity profiles obtained were compared with those computed using a CTR central differencing LES code. The dynamic SGS model is found to have little effect when there is a large amount of numerical dissipation as in the case of the 5th order scheme. We have found in this study that the 9th and 11th order schemes have relatively small numerical dissipation so that the dynamic SGS model plays a significant role. In order to improve cost effectiveness of LES for practical applications, a RANS type wall model was also implemented. Although the velocity profile obtained using LES in conjunction with the wall model agrees well with the one obtained using the full LES calculation, the magnitude of the pressure fluctuation was found to be higher.

REFERENCES

Boersma B. J. & Lele S. K. 1999 Large eddy simulation of compressible turbulent jets. *Annual Research Briefs,* Center for Turbulence Research, NASA Ames/Stanford Univ. 265-377.

Cabot, W. & Moin P. 2000 Approximate wall boundary conditions in the Large-eddy simulation of high Reynolds number flow. *J. Flow, Turbulence & Combustion*. **63**, 269-291.

Choi D., Barber T. J. & Chiappetta, L. M. 1999 Large Eddy Simulation of high Reynolds number jet flows. *AIAA Paper 99-0230.*

Germano, M. Piomelli, U., Moin, P. & Cabot, W. H. 1991 A dynamic subgrid-scale eddy viscosity model. *Phys. Fluids A.* **3**, 1760-1765.

Lilly, D. K. 1992 A proposed modification of Germano's subgrid-scale closure method. *Phys. Fluids A.* **4**, 633-635.

Madabhushi, R. K. , Choi D. & Barber T. J. 1997 Unsteady simulations of turbulent flow behind a triangular bluff body. *AIAA Paper 97-3182.*

Moin, P., Squires, K., Cabot, W. & Lee, S. 1991 Dynamic subgrid-scale model for compressible turbulence and scalar transport. *Phys. Fluids A.* **3**, 2746-2757.

Wake, B. E. & Choi, D. 1996 Investigation of high-order upwinded differencing for vortex convection. *AIAA Paper 95-1719.*

Wang, M. 1999 LES with wall models for trailing-edge aeroacoustics. *Annual Research Briefs,* Center for Turbulence Research, NASA Ames/Stanford Univ. 355-364.